Université Catholique de Louvain

2021-2022

LACTU-2170
Project in stochastic finance : pricing of derivatives

Students

Maxime Druez (8754-21-00)

Hugo Léal (1847-21-00)

Professor

Donatien Hainaut

May 2, 2022

Contents

"When your price is very high, people assume that your product must be very good!"

1 Introduction

This work aims to implement various techniques seen in class for the pricing of derivatives. In section 2, we will focus on Monte Carlo (MC) numerical simulations in order to price a European put option exerted on a basket of two stocks, with a knock-out condition. The simple market model (with only two risky assets) will be calibrated based on historical volatilities. In section 3, three pricing techniques will be applied on a European call option exerted on a commodity (following a mean reverting dynamics under the risk neutral measure): analytical pricing - trinomial trees - Monte Carlo simulations. All along this report, we will try to compare the advantages and disadvantages of the various pricing methodologies envisioned.

2 Question I: European put option on a basket with knock-out condition

2.1 Problem statement and market assumptions

On February 4, 2022 (time $t = 0$), we wish to price a European put option of maturity $T = 2$ years on an equi-weighted basket of Amazon and Alphabet stocks (whose prices are respectively denoted $(S_t^1)_{t\geq 0}$ and $(S_t^2)_{t\geq 0}$ for any time $t \in \mathbb{R}^+$). We will consider the following simple model (under the real measure $\mathbb{P}$) for the market, only containing those two risky assets (S_t^1 and S_t^2) in addition to the cash account B_t earning the risk-free rate r:

$$\begin{pmatrix} \frac{dS_t^1}{S_t^1} \\ \frac{dS_t^2}{S_t^2} \end{pmatrix} = \begin{pmatrix} \mu_1 \\ \mu_2 \end{pmatrix} dt + \begin{pmatrix} \sigma_{11} & \sigma_{12} \\ \sigma_{21} & \sigma_{22} \end{pmatrix} \begin{pmatrix} dW_t^1 \\ dW_t^2 \end{pmatrix} = \bar{\mu} dt + \Sigma \begin{pmatrix} dW_t^1 \\ dW_t^2 \end{pmatrix} \qquad dB_t = rB_t dt \qquad [II.1]$$

where $\bar{\mu}$ and Σ are constant real matrices and where W_t^1 and W_t^2 are independent brownian motions under $\mathbb{P}$. At $t = 0$, we have $S_0^1 = 3103.5\$$ and $S_0^2 = 2849.35\$$. The risk free rate r (continuous compounded an annual basis) will be supposed to remain constant. The swap rate at time t=0 (horizon two years which is the maturity of the option) will be considered as a proxy for this r value. We will thus take $r = 1.49\%$. Per default, all equations and constants will be expressed in years.

At time $t = T = 2y.$, the payoff of the put option is $\left(K - (S_T^1 + S_T^2)\right)_+$ where the strike K ranges from 5000\$ to 7000\$ by steps of 200\$. We consider a knock-out condition: if the value of the basket falls below 80% of the strike K, the option expires. Equivalently, in such a case where the barrier is exceeded, the payoff of the option is null. We wish to compute the price $P(0, S_0^1, S_0^2, K)$ of this put derivative at time $t = 0$ with knock-out condition.

2.2 Model calibration: historical variances and covariances

The parameters of the model [II.1] must be calibrated. The pricing methodology, applied in section 2.3, will rely on the risk neutral measure, where the drifts of both assets will be set to the risk free rate r. In fact, the price of the option will be totally independent of the drifts μ_1 and μ_2 in force under the real measure. As such, only the variance-covariance part of the model must be evaluated.

A possible way to calibrate the model would rely on an analytical formula for the price of the derivative and would adjust implicit volatilities *via* available market prices. In the present case, it is not asked to develop a closed expression for the put price. In fact, it is doubtful that such an explicit form exists due to the barrier condition. Besides, the market for such an option is dry and few market prices are available. This is why the model will rather be adjusted based on historical volatilities and covariances of Amazon and Alphabet stocks. By doing so, we assume that future variances and covariances will behave (at least during the next two years) just as the historical ones (that are based on past observations). We neglect in our model time-varying parameters and future shocks on the market. The historical matrix of variances-covariances will be computed using the files AMZN.csv and GOOG.csv (retrieved from the Moodle website) that contain daily quotes from the 4/2/21 to the 4/2/22.

It was demonstrated in class (using Itô's lemma cf. slides 143-144 of the course), that under $\mathbb{P}$, for the model [II.1], the vector of log returns follows a bivariate normal variable:

$$\begin{pmatrix} \ln\left(\frac{S_t^1}{S_0^1}\right) \\ \ln\left(\frac{S_t^2}{S_0^2}\right) \end{pmatrix} \overset{d,\mathbb{P}}{=} \mathcal{N}\left[[\bar{\mu} - \frac{1}{2}\text{diag}(\Sigma\Sigma^T)]t, \Sigma\Sigma^T t \right] \qquad [II.2]$$

From [II.2] (where the time units are expressed in years) and assuming that the year counts 255 days of trading, we also see that the daily covariance matrix is simply related to the yearly covariance matrix by a factor $\frac{1}{255}$. In other words, it is sufficient to estimate the daily covariance matrix. Its multiplication by 255 delivers the yearly covariance matrix, whose Choleski's decomposition reduces in turn to Σ.

From the csv files of daily quotes, both series of daily log-returns were computed (log of the quotient of successive closing records). We assumed log-returns indeed following a bivariate normal distribution and we supposed serial independence between successive records (both hypotheses are heavily disputable). In consequence, the R-functions `var` and `cov` were applied on those samples of daily log-returns in order to estimate the historical daily covariance matrix. The multiplication by the factor 255 delivers the following yearly covariance matrix:

$$M = \begin{pmatrix} 0.08149785 & 0.03817844 \\ 0.03817844 & 0.05557192 \end{pmatrix} \qquad [II.3]$$

On the diagonal, we find the yearly variances of log-returns whereas the yearly covariance corresponds to the off-diagonal elements. This amounts to a yearly standard deviation of 28.5478% for the Amazon log-returns (labelled 1), of 23.5737% for the Alphabet log-returns (labelled 2) and to a correlation of 56.7306%. The Choleski's decomposition of [II.3] finally delivers the required parameters in [II.1]: $\sigma_{11} = 0.2854783$, $\sigma_{12} = 0.1337350$, $\sigma_{21} = 0$, $\sigma_{22} = 0.1941311$.

2.3 Pricing with Monte Carlo simulation: methodology

It was natural to adjust the model [II.1], defined under the real measure $\mathbb{P}$, using historical data. However, the pricing of the basket European put option will be conducted under the risk neutral framework. Since the market includes three assets (S_t^1, S_t^2, B_t) and two risk factors (W_t^1, W_t^2), it is complete and there exists a unique risk neutral measure $\mathbb{Q}$. Under $\mathbb{Q}$, the dynamics of the stocks will exhibit a risk neutral drift (cf. appendix B):

$$\begin{pmatrix} \frac{dS_t^1}{S_t^1} \\ \frac{dS_t^2}{S_t^2} \end{pmatrix} = \begin{pmatrix} r \\ r \end{pmatrix} dt + \begin{pmatrix} \sigma_{11} & \sigma_{12} \\ \sigma_{21} & \sigma_{22} \end{pmatrix} \begin{pmatrix} dW_t^{1\mathbb{Q}}, \\ dW_t^{2\mathbb{Q}} \end{pmatrix} \qquad [II.4]$$

where $W_t^{1\mathbb{Q}}$ and $W_t^{2\mathbb{Q}}$ are independent brownian motions under $\mathbb{Q}$. Let us note that the drifts μ_1 and μ_2 of [II.1] have disappeared from the computations and that the option prices will be independent of those quantities.

A Monte Carlo (MC) simulation (or MC run) is defined by a number N of scenarios (or paths), upon which the averaging will be performed, and by a constant time step Δt for the sampling. Within a MC run, N paths are sampled for the underlying stocks by exploiting their risk neutral dynamics [II.4]. Since $W_t^{1\mathbb{Q}}$ and $W_t^{2\mathbb{Q}}$ are independent brownian motions under $\mathbb{Q}$, with independent successive increments (normally distributed, with zero mean and variance proportional to time), a discrete time version of the risk neutral dynamics [II.4] is given by:

$$\Delta S^{1,(i)}(j) = rS^{1,(i)}(j-1)\Delta t + \sigma_{11}S^{1,(i)}(j-1).\sqrt{\Delta t}.u^{1,(i)}(j) + \sigma_{12}S^{1,(i)}(j-1).\sqrt{\Delta t}.u^{2,(i)}(j) \qquad [II.5]$$

$$\Delta S^{2,(i)}(j) = rS^{2,(i)}(j-1)\Delta t + \sigma_{21}S^{2,(i)}(j-1).\sqrt{\Delta t}.u^{1,(i)}(j) + \sigma_{22}S^{2,(i)}(j-1).\sqrt{\Delta t}.u^{2,(i)}(j) \qquad [II.6]$$

$$S^{1,(i)}(j) = S^{1,(i)}(j-1) + \Delta S^{1,(i)}(j) \qquad S^{2,(i)}(j) = S^{2,(i)}(j-1) + \Delta S^{2,(i)}(j) \qquad [II.7]$$

for $j = 1, 2, ..., \frac{T}{\Delta t}$, starting from $S^{1,(i)}(0) = S_0^1$ and $S^{2,(i)}(0) = S_0^2$ and where $u^{1,(i)}(j)$ and $u^{2,(i)}(j)$ are independent random samples from a $\mathcal{N}(0,1)$. This sampling is performed for each scenario $i = 1, 2, ..., N$. Even if the two brownian motions $W_t^{1\mathbb{Q}}$ and $W_t^{2\mathbb{Q}}$ are independent, the correlation between the two stocks is accounted for *via* the Σ matrix.

For any scenario $i = 1, 2, ..., N$, the knock-out condition can be evaluated at any discrete time instant $j\Delta t$ for $j = 1, 2, ..., \frac{T}{\Delta t}$:

$$S^{1,(i)}(j) + S^{2,(i)}(j) \leq 0.8K \qquad [II.8]$$

If it is exceeded, we know that the option will not be exerted at maturity. It is useless to pursue the sampling of that scenario i. In other words, the option payoff $P^{(i)}$ for that scenario i can be set to zero and one can go to the sampling of the next scenario (i+1).

Otherwise, for a scenario i, if the barrier condition is not encountered before the maturity T, the payoff $P^{(i)}$ for that scenario i at maturity T will be:

$$P^{(i)} = \left[K - \left(S^{1,(i)}(j = \frac{T}{\Delta t}) + S^{2,(i)}(j = \frac{T}{\Delta t})\right)\right]_+ \qquad [II.9]$$

A MC run produces thus N sampled option payoffs $P^{(i)}$ at maturity (for $i = 1, 2, ..., N$). This sample distribution approximates the true risk neutral distribution of the put payoff at maturity. As such, in the fundamental theorem of asset pricing, the expectation over $\mathbb{Q}$ can be replaced by a sample average over the N sampled payoffs (discounted at the risk free rate):

$$P(0, S_0^1, S_0^2, K) = \mathbb{E}^{\mathbb{Q}}\left[e^{-rT}\left(K - (S_T^1 + S_T^2)\right)_+ | \mathscr{F}_0\right] \approx \frac{1}{N}\sum_{i=1}^{N} e^{-rT} P^{(i)} \qquad [II.10]$$

Since the knock-out condition must be followed over time for any scenario $i = 1, 2, ..., N$, we are forced to consider a discrete time implementation with a finite Δt. This will require a double convergence study (for the time step $\Delta t \to 0$ and for the number of scenarios $N \to +\infty$).

The sample average [II.10] could be computed by storing all the payoffs $P^{(i)}$ (for $i = 1, 2, ..., N$), by performing the summation and then dividing by N. However, this is not practical numerically for $N \to +\infty$. This would indeed increase the memory requirements and the result of the summation could exceed the internal numerical representation of the computer for N large enough. This is why the average is computed in a more efficient fashion:

$$MC(k{+}1) = \frac{1}{k+1}\sum_{i=1}^{k+1} e^{-rT} P^{(i)} = \frac{1}{k+1}\left[k.\frac{1}{k}\sum_{i=1}^{k} e^{-rT} P^{(i)} + e^{-rT} P^{(k+1)}\right] = \frac{1}{k+1}\left[k.MC(k) + e^{-rT} P^{(k+1)}\right] [II.11]$$

Only one value must be stored (the MC estimator MC(k) based on the k first paths sampled). MC(k) can be updated progressively as the paths are sampled (for $k = 1, 2, ..., N$). MC(N) is equivalent to [II.10] and MC(k) does not explode in value for large N.

2.4 Pricing with Monte Carlo simulation: results and convergence

As mentioned in section 2.3, a double convergence study must be carried out (for $\Delta t \to 0$ and for $N \to +\infty$). Strictly speaking, one should perform those two studies simultaneously. In practice, the convergence in N is studied first for a small enough Δt. It allows to find the number N of scenarios that is appropriate considering the precision requirements. Then, the convergence in Δt is studied for a N large enough. It allows to find the time step Δt that is appropriate considering the precision requirements. We will then assume that the N and Δt found in this manner remains adequate (w.r.t. the precision requirements) when they are used concomitantly.

1. Convergence in N (number of scenarios)
Such a convergence study in N is illustrated in fig. 1. It was conducted for a particular strike K=6000$, for the price of the basket European put option at time t = 0 (February 04, 2022) and for the calibrated parameters of section 2.2. For a small enough $\Delta t = 0.01$y., several MC runs were performed using various numbers N of scenarios. As N grows, the computation time is increasing. Since the MC simulation exploits stochastic sampling, for a definite N and a given Δt, some dispersion might still occur across different MC runs. This is why for any N studied, ten MC runs were envisioned, to assess the level of convergence.

In fig. 1, one can indeed notice that the numerical MC price seems to converge as N is increasing. The residual dispersion across the MC runs using a given N is reduced for a larger N. Also, the mean price across the MC runs seems to stabilise, as illustrated by the dotted line in fig. 1. This is not yet the converged MC price as the convergence in Δt has not been studied yet.

The convergence appears to be rather slow, probably due to the two risk factors (W_t^1, W_t^2), due to the long time horizon ($T = 2$y.) and due to the necessity to assess the knock-out condition over time for any scenario. In any case, it is well known that the convergence of MC simulation is driven by $1/\sqrt{N}$. Here, for $N = 50,000$ scenarios, the residual dispersion of the ten MC runs around their mean is still about the unity. Depending on the degree of convergence required, one could select the appropriate N, above which the residual dispersion is consistent w.r.t. the desired precision.

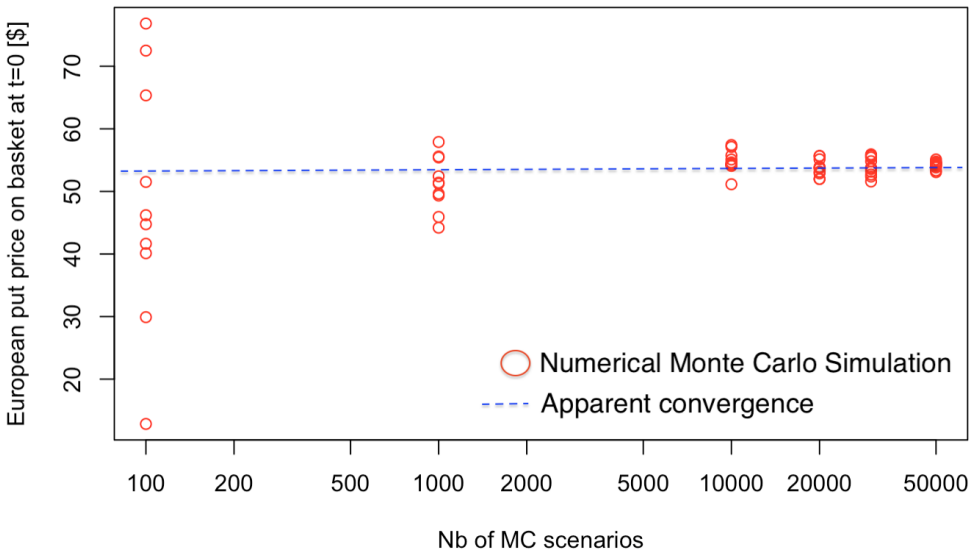

Figure 1: For a strike K=6000$ and for the calibrated parameters of section 2.2, numerical MC price of the basket European put option at time t = 0 (February 04, 2022), as a function of the number N of scenarios for the MC simulation.

2. Convergence in Δt (time step)

Such a convergence study in Δt was illustrated in fig. 2. It was conducted for a particular strike K=6000$, for the price of the basket European put option at time t = 0 (February 04, 2022) and for the calibrated parameters of section 2.2. For a large enough N = 20,000, several MC runs were performed using various time steps Δt. As Δt is reduced, the computation time is increasing. Since the MC simulation exploits stochastic sampling, for a definite N and a given Δt, some dispersion might still occur across different MC runs. This is why for any Δt studied, ten MC runs were envisioned, to assess the level of convergence.

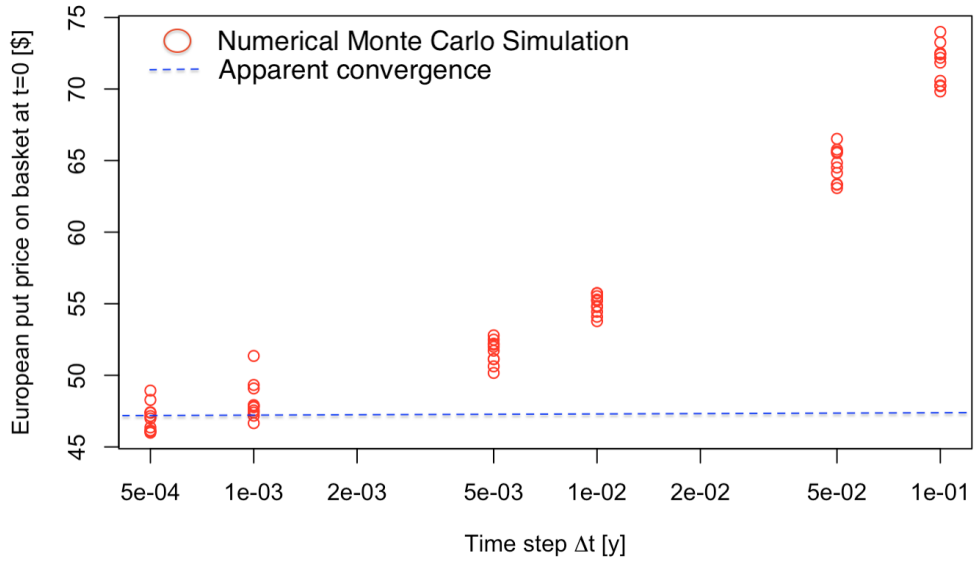

Figure 2: For a strike K=6000$ and for the calibrated parameters of section 2.2, numerical MC price of the basket European put option at time t = 0 (February 04, 2022), as a function of the time step Δt for the MC simulation.

The main effect of Δt lies in the mean level around which the ten MC runs are dispersed. In fig. 2, one can indeed notice that the mean level across the ten MC runs seems to converge towards a stable level (highlighted by the dotted line) as Δt is reduced. This is an expected result as the discrete time approximations [II.5-7] should converge towards the continuous case for a smaller Δt. Also, when Δt is reduced, the barrier condition is checked more frequently. This gives somehow more opportunities to assess a violation of the knock-out condition for smaller Δt, until this phenomenon saturates when the convergence occurs. Since the option is not exerted at maturity for a violation of the barrier condition, this naturally decreases the price of the option as noticed in fig. 2, until the convergence occurs at small Δt. In particular, this is why such a barrier condition could be envisioned on such a derivative: to reduce its price. Depending on the degree of convergence required, one could select the appropriate Δt, under which the mean MC indicator is consistent w.r.t. the desired precision.

3. Converged results

Finally, one can plot the converged MC numerical prices $P(0, S_0^1, S_0^2, K)$ for the basket European put option at time t = 0 (February 04, 2022) and for the calibrated parameters of section 2.2. This was done in fig. 3, for several strikes. In any case, we used $N = 50,000$ scenarios and $\Delta t = 0.0005$y.. We assume here that the convergence is appropriate for any strike level studied and when the N and Δt parameters are combined. Strictly speaking, the degree of convergence reached could be different for any change in the parameters (including the strike). One would have to properly assess the level of convergence in all those cases with a separate convergence study.

A curve with negative concavity seems to emerge from the computations. This can be explained from the characteristics of the product we wish to price. On one hand, the payoff of the put option is increased for a bigger strike K. This tends to increase the price of the derivative as K is growing. On the other hand, the knock-out condition is more easily reached for a bigger strike. Since the option is not exerted at maturity when the barrier is met, this tends to decrease the price of the derivative as K is growing. From those two opposite mechanisms, it seems natural to observe a maximum for the price of the derivative as K is varying.

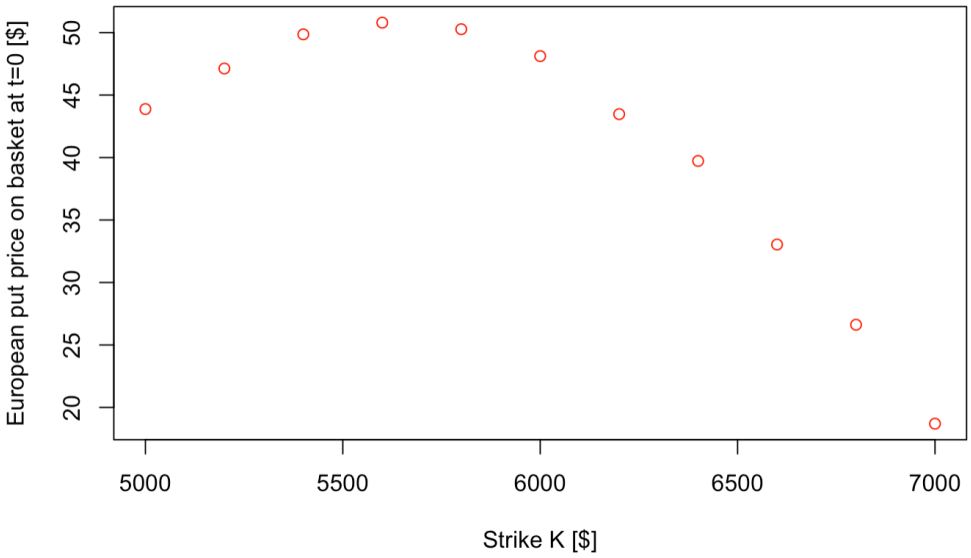

Figure 3: For several strikes K and for the calibrated parameters of section 2.2, numerical MC price of the basket European put option at time t = 0 (February 04, 2022), for $N = 50,000$ scenarios and $\Delta t = 0.0005$y..

3 Question II: European call option on a mean reverting commodity

3.1 Problem statement

On February 4, 2022 (time $t = 0$), we wish to price a European call option of maturity $T = 1$y. (12 months) on the barrel of oil (whose price is denoted S_t for any time $t \in \mathbb{R}^+$). This underlying commodity follows a mean reverting dynamics (Ornstein-Uhlenbeck process) under the risk neutral measure $\mathbb{Q}$:

$$dS_t = \alpha(\theta - S_t)dt + \sigma dW_t \qquad [III.1]$$

where W_t is a brownian motion under $\mathbb{Q}$ and where $\alpha = 0.90y^{-1}$, $\theta = 92\$$ and $\sigma = 15\$$. At $t = 0$, we have $S_0 = 92.81\$$. The market contains a cash account B_t earning the risk-free rate $r = 1.03\%$ (continuous compounded on annual basis, assumed to remain constant):

$$dB_t = rB_t dt \qquad [III.2]$$

Per default, all equations and constants will be expressed in years.

At time $t = T = 1$y., the payoff of the call option is $(S_T - K)_+$ where the strike K ranges from 70\$ to 110\$. For any such strike and for $t \in [0, 1]$, we must compute the price $C(t, S_t, K)$ of the call derivative.

3.2 Analytical price

To solve equation [III.1], let us define the process Z_t such that

$$Z_t = e^{\alpha t}(\theta - S_t) \iff S_t = \theta - e^{-\alpha t}Z_t \iff e^{-\alpha t}Z_t = (\theta - S_t) \qquad [III.3]$$

Applying Itô's lemma and substituting with equation [III.1], we obtain:

$$dZ_t = \alpha e^{\alpha t}(\theta - S_t)dt - e^{\alpha t}dS_t = \alpha e^{\alpha t}(\theta - S_t)dt - e^{\alpha t}[\alpha(\theta - S_t)dt + \sigma dW_t] = -\sigma e^{\alpha t}dW_t \qquad [III.4]$$

For $0 \leq s \leq t \leq T$, the integration w.r.t. time delivers

$$Z_t = Z_s - \sigma \int_s^t e^{\alpha u}dW_u \qquad [III.5]$$

Combining equations [III.3] and [III.5], we can express the commodity price

$$\begin{aligned} S_t &= \theta - e^{-\alpha t}Z_t = \theta - e^{-\alpha t}\left[Z_s - \sigma \int_s^t e^{\alpha u}dW_u\right] = \theta - e^{-\alpha t}e^{\alpha s}e^{-\alpha s}Z_s + \sigma \int_s^t e^{-\alpha(t-u)}dW_u \\ &= \theta - e^{-\alpha(t-s)}(\theta - S_s) + \sigma \int_s^t e^{-\alpha(t-u)}dW_u \\ &= e^{-\alpha(t-s)}S_s + \theta[1 - e^{-\alpha(t-s)}] + \sigma \int_s^t e^{-\alpha(t-u)}dW_u \qquad [III.6] \end{aligned}$$

Since W_t is a brownian motion under $\mathbb{Q}$, the last term in [III.6] is an Itô's integral. As such, it is a martingale under $\mathbb{Q}$. It is also gaussian, with zero mean

$$\mathbb{E}^{\mathbb{Q}}\left[\sigma \int_s^t e^{-\alpha(t-u)}dW_u|\mathscr{F}_s\right] = 0 \qquad [III.7]$$

Its variance can be retrieved from Itô's property of isometry:

$$\begin{aligned} \mathbb{V}^{\mathbb{Q}}\left[\sigma \int_s^t e^{-\alpha(t-u)}dW_u|\mathscr{F}_s\right] &= \sigma^2 e^{-2\alpha t}\mathbb{V}^{\mathbb{Q}}\left[\int_s^t e^{\alpha u}dW_u|\mathscr{F}_s\right] = \sigma^2 e^{-2\alpha t}\mathbb{E}^{\mathbb{Q}}\left[(\int_s^t e^{\alpha u}dW_u)^2|\mathscr{F}_s\right] \\ &= \sigma^2 e^{-2\alpha t}\int_s^t e^{2\alpha u}du = \frac{\sigma^2}{2\alpha}[1 - e^{-2\alpha(t-s)}] \qquad [III.8] \end{aligned}$$

As such, under $\mathbb{Q}$ and seen from s ($0 \leq s \leq t \leq T$), the commodity price S_t is normally distributed:

$$S_t \overset{d,\mathbb{Q}}{=} \mathscr{N}\left[e^{-\alpha(t-s)}S_s + \theta(1-e^{-\alpha(t-s)}), \frac{\sigma^2}{2\alpha}(1-e^{-2\alpha(t-s)})\right] \qquad [III.9]$$

In other words, under $\mathbb{Q}$ and seen from t ($0 \leq t \leq T$), the commodity price S_T at maturity is normally distributed:

$$\begin{aligned} S_T &\overset{d,\mathbb{Q}}{=} \mathscr{N}\left[e^{-\alpha(T-t)}S_t + \theta(1-e^{-\alpha(T-t)}), \frac{\sigma^2}{2\alpha}(1-e^{-2\alpha(T-t)})\right] \\ &\overset{d,\mathbb{Q}}{=} d_1 + d_2 u \qquad [III.10] \end{aligned}$$

where $u \overset{d,\mathbb{Q}}{=} \mathscr{N}(0,1)$ and where $d_1 = e^{-\alpha(T-t)}S_t + \theta(1-e^{-\alpha(T-t)})$ and $d_2 = \frac{\sigma}{\sqrt{2\alpha}}\sqrt{1-e^{-2\alpha(T-t)}}$.

The fundamental theorem of asset pricing allows then to price the European call option on the barrel of oil. Under the risk neutral measure $\mathbb{Q}$, the price of the derivative (discounted at the risk free rate) is a martingale. It follows:

$$\begin{aligned} C(t,S_t,K) &= \mathbb{E}^{\mathbb{Q}}\left[e^{-r(T-t)}(S_T-K)_+|\mathscr{F}_t\right] = \int_{d_1+d_2u\geq K}^{+\infty} e^{-r(T-t)}(d_1+d_2u-K)\frac{1}{\sqrt{2\pi}}e^{-u^2/2}du \\ &= e^{-r(T-t)}\left[d_2\int_{\frac{K-d_1}{d_2}}^{+\infty} u\frac{1}{\sqrt{2\pi}}e^{-u^2/2}du - (K-d_1)\int_{\frac{K-d_1}{d_2}}^{+\infty}\frac{1}{\sqrt{2\pi}}e^{-u^2/2}du\right] \qquad [III.11] \end{aligned}$$

The two integrals in [III.11] can be computed easily. If ϕ denotes the cdf of a standard $\mathscr{N}(0,1)$, we obtain:

$$\int_{\frac{K-d_1}{d_2}}^{+\infty}\frac{1}{\sqrt{2\pi}}e^{-u^2/2}du = \phi\left[\frac{d_1-K}{d_2}\right] \qquad [III.12]$$

$$\int_{\frac{K-d_1}{d_2}}^{+\infty} u\frac{1}{\sqrt{2\pi}}e^{-u^2/2}du \overset{w=u^2/2}{=} \int_{\frac{1}{2}(\frac{K-d_1}{d_2})^2}^{+\infty}\frac{1}{\sqrt{2\pi}}e^{-w}dw = \frac{1}{\sqrt{2\pi}}exp\left[-\frac{1}{2}\left(\frac{K-d_1}{d_2}\right)^2\right] \qquad [III.13]$$

Combining equations [III.11], [III.12] and [III.13], we finally obtain an analytical expression for the price of the derivative:

$$C(t,S_t,K) = e^{-r(T-t)}\left[\frac{d_2}{\sqrt{2\pi}}exp\left[-\frac{1}{2}\left(\frac{K-d_1}{d_2}\right)^2\right] - (K-d_1)\phi\left[\frac{d_1-K}{d_2}\right]\right] \qquad [III.14]$$

$$\text{where} \qquad d_1 = e^{-\alpha(T-t)}S_t + \theta(1-e^{-\alpha(T-t)}) \qquad \text{and} \qquad d_2 = \frac{\sigma}{\sqrt{2\alpha}}\sqrt{1-e^{-2\alpha(T-t)}}$$

In particular, for a pricing at time $t = 0$:

$$C(0,S_0,K) = e^{-rT}\left[\frac{d_2}{\sqrt{2\pi}}exp\left[-\frac{1}{2}\left(\frac{K-d_1}{d_2}\right)^2\right] - (K-d_1)\phi\left[\frac{d_1-K}{d_2}\right]\right] \qquad [III.15]$$

$$\text{where} \qquad d_1 = e^{-\alpha T}S_0 + \theta(1-e^{-\alpha T}) \qquad \text{and} \qquad d_2 = \frac{\sigma}{\sqrt{2\alpha}}\sqrt{1-e^{-2\alpha T}}$$

For the parameters given in section 3.1, the analytical price [III.15] of the European call option on the barrel of oil, at time $t = 0$ (February 04, 2022), was plotted as a function of the strike in fig. 4. As expected from a call option, the price is decreasing with the strike K since the payoff at maturity is decreasing with K.

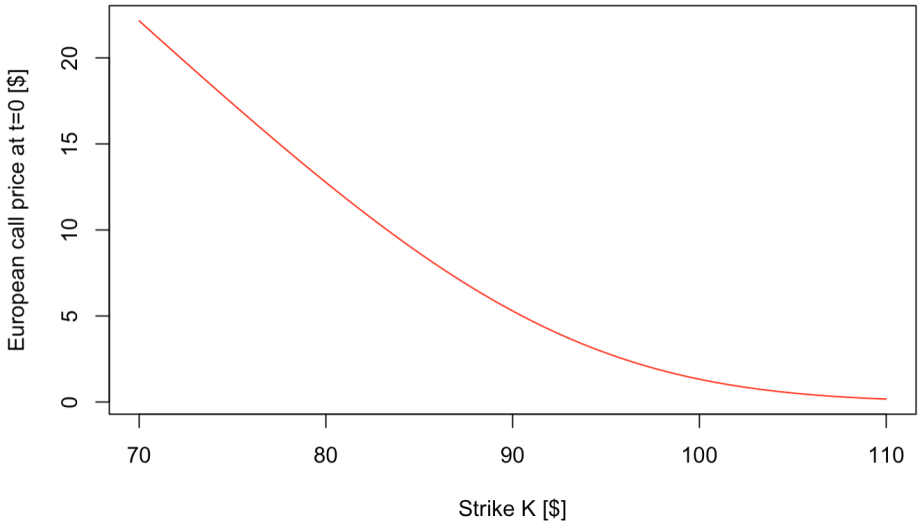

Figure 4: For the parameters given in section 3.1, the analytical price [III.15] of the European call option on the barrel of oil, at time $t = 0$ (February 04, 2022) as a function of the strike K.

3.3 Trinomial tree pricing methodology and convergence

We will now price numerically the European call option on the mean reverting commodity by implementing a trinomial tree. This section was heavily inspired by chapter 31 of Hull's reference work "Options, Futures and Other Derivatives" [1] that will be referred to as [HULL] in what follows. [HULL] develops a tree building procedure to price interest rate derivatives relying on a Vasicek model for the short rate. The problem is mathematically equivalent to the one explored in this section 3 since the mean reverting dynamics for the barrel of oil remains similar on all aspects w.r.t. the Vasicek model. *"It often proves to be convenient to use a trinomial rather than a binomial tree [...]. It provides an extra degree of freedom, making it easier for the tree to represent features [...] such as mean reversion"* [HULL]. The pricing methodology is essentially a three steps procedure.

3.3.1 Pricing methodology

1. Build a tree for the related process S_t^*
Our final objective will be the construction of a tree (discrete time representation) for the process S_t (price of the barrel) obeying the dynamics of equation [III.1]. However, [HULL] proposes first to build a tree for the related process S_t^* (initially $S_0^* = 0$) following the dynamics

$$dS_t^* = -\alpha S_t^* dt + \sigma dW_t \qquad [III.16]$$

We will suppose the time step Δt of the tree to be constant. We define $\Delta S = \sigma\sqrt{3\Delta t}$. *"This proves to be a good choice of ΔS from the viewpoint of error minimization"* [Hull].

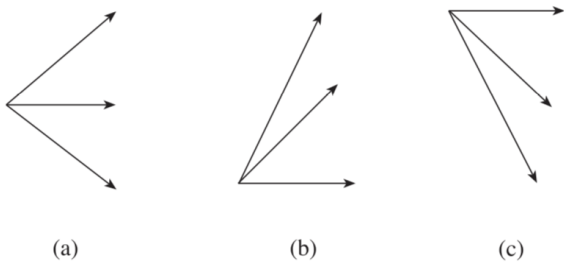

Figure 5: Three branching alternatives for the trinomial tree.

[1] Hull, J. C.. Options, Futures and other derivatives. Ninth edition. Pearson Education, 2015. Chapter 31: Interest rate derivatives: Models of the short rate. Sections 31.6 and 31.7 about interest rate trees. pp 721-732.

A trinomial tree for S_t^* will be an ensemble of nodes (i,j) where $t = i\Delta t$ ($i = 0, 1, ..., N = \frac{T}{\Delta t}$) and where $S^* = j\Delta S$ (j is a positive or negative integer ranging from j_{min} to j_{max}). Starting from the initial node (0,0) (where $t = 0$ and $S^* = 0$), the tree develops itself in a discrete time representation of S_t^*. One must define for each node the branching method that will be used as well as the probabilities associated to each branch. *"The branching method used must lead to the probabilities on all three branches being positive"* [Hull], for any node.

Three alternatives can be elicited for the branching method. They are shown in fig. 5. The branching (a) will be called the usual branching. For most nodes, this will be the appropriate branching method. Yet, *"since $\alpha > 0$, it is necessary to switch from branching (a) to branching (c) for a sufficiently large j, to incorporate mean reversion when S^* is sufficiently large. Similarly, it is necessary to switch from branching (a) to branching (b) for j negative enough, to incorporate mean reversion when S^* is sufficiently low"* [HULL]. Branching (b) will be called an upward branching whereas branching (c) will be called a downward branching. The switching from branching (a) towards branching (c) occurs when $j = j_{max}$ and the one towards branching (b) occurs when $j = j_{min}$. *"Probabilities are always positive if j_{max} is set equal to the smallest integer greater than $\frac{0.184}{\alpha\Delta t}$ and j_{min} is set equal to $-j_{max}$"* [HULL].

The previous considerations define entirely the branching of the trinomial tree for S_t^*. However, the branching probabilities remain to be defined. *"Let us define $p_u(i,j)$, $p_m(i,j)$ and $p_d(i,j)$ as the probabilities of the highest, middle, and lowest branches emanating from the node (i,j). Those probabilities are chosen to match the expected change as well as the variance of the change in S^* over the next time interval Δt. The probabilities must also sum to unity. This leads to three equations in the three probabilities."* [HULL].

Considering [III.16] and neglecting higher order terms than Δt, we have

$$S^*(t+\Delta t) - S^*(t) \overset{d,\mathbb{Q}}{=} \mathscr{N}\left[-\alpha S^*(t)\Delta t, \sigma^2\Delta t\right] \qquad [III.17]$$

As such, if the node (i,j) corresponds to an usual branching (a), the three conditions (on the expectation and variance of the change as well as the summation of probability toward the unity) lead to the system:

$$\begin{aligned} p_u(i,j)\Delta S - p_d(i,j)\Delta S &= -\alpha j \Delta S \Delta t \\ p_u(i,j)\Delta S^2 + p_d(i,j)\Delta S^2 &= \sigma^2\Delta t + \alpha^2 j^2 \Delta S^2 \Delta t^2 \\ p_u(i,j) + p_m(i,j) + p_d(i,j) &= 1 \end{aligned} \qquad [III.18]$$

For $\Delta S = \sigma\sqrt{3\Delta t}$, the solution is given by:

$$p_u(i,j) = \frac{1}{6} + \frac{1}{2}(\alpha^2 j^2 \Delta t^2 - \alpha j \Delta t) \qquad p_m(i,j) = \frac{2}{3} - \alpha^2 j^2 \Delta t^2 \qquad p_d(i,j) = \frac{1}{6} + \frac{1}{2}(\alpha^2 j^2 \Delta t^2 + \alpha j \Delta t) \qquad [III.19]$$

For an upward branching (b), a similar reasoning leads to

$$p_u(i,j) = \frac{1}{6} + \frac{1}{2}(\alpha^2 j^2 \Delta t^2 + \alpha j \Delta t) \quad p_m(i,j) = \frac{-1}{3} - \alpha^2 j^2 \Delta t^2 - 2\alpha j \Delta t \quad p_d(i,j) = \frac{7}{6} + \frac{1}{2}(\alpha^2 j^2 \Delta t^2 + 3\alpha j \Delta t) \quad [III.20]$$

For a downward branching (c), a similar reasoning leads to

$$p_u(i,j) = \frac{7}{6} + \frac{1}{2}(\alpha^2 j^2 \Delta t^2 - 3\alpha j \Delta t) \quad p_m(i,j) = \frac{-1}{3} - \alpha^2 j^2 \Delta t^2 + 2\alpha j \Delta t \quad p_d(i,j) = \frac{1}{6} + \frac{1}{2}(\alpha^2 j^2 \Delta t^2 - \alpha j \Delta t) \quad [III.21]$$

In order to verify this first stage of the procedure, one can check that the S^* values are symmetrical (up to a minus sign) around the median line of the tree ($j = 0$), that the probabilities only depend on j (not on i) and that probabilities are mirrored around the median line.

2. Offset the previous tree to get a discrete time representation of S_t

"The second stage in the tree construction is to convert the tree for S_t^* into a tree for S_t" [HULL]. It requires to compute the offset process

$$q_t = S_t - S_t^* \quad \text{with} \quad q_0 = S_0 - S_0^* = S_0 \qquad [III.22]$$

Since [HULL] works with interest rates, he wishes to match perfectly their initial term structures for a finite Δt. In order to do so, he uses an iterative procedure to compute the q_t's in force at the different nodes and disregards the analytical solution for this offset. Here, as there is no such consideration of term matching for the commodity price process, we can use in a straight forward manner the analytical solution of q_t to offset the trinomial tree. Indeed, from [III.1], [III.16] and [III.22], we retrieve immediately

$$dq_t = dS_t - dS_t^* = \alpha(\theta - q_t)dt \quad \text{with} \quad q_0 = S_0 \qquad [III.23]$$

The solution of this classical differential equation is trivially given by

$$q_t = S_0 e^{-\alpha t} + \theta(1 - e^{-\alpha t}) \qquad [III.24]$$

As such, the branching structures and the branching probabilities are just about the same for the S^* and S trees. The only difference lies in the values of the related processes S^* and S at any node. For the S^*-tree, the node (i,j) corresponds to $t = i\Delta t$ and $S^*(i,j) = j\Delta S$. Accounting for the offset, in the S-tree, the same node (i,j) still corresponds to $t = i\Delta t$ but is now associated to $S(i,j) = S^*$(i,j) + offset $= S^*(i,j) + q(i\Delta t) = j\Delta S + S_0 e^{-\alpha i \Delta t} + \theta(1 - e^{-\alpha i \Delta t})$.

3. Price the European call option on the mean reverting commodity

The tree obtained at the end of the second stage is a discrete time representation of the process S_t in the risk neutral world, as seen from the instant defining the initial node (0,0). In particular, the branching probabilities that we computed previously are risk neutral probabilities. Indeed, the trees of first and second stages were built based on equations [III.1] and [III.16] defining risk neutral dynamics. As such, the values of S obtained at the terminal nodes of the S-tree (corresponding to the maturity $t = T$ of the option) can be used to compute a risk neutral and discrete representation of the derivative's payoff. At the terminal node $(i = \frac{T}{\Delta t}, j)$, the call payoff is given by:

$$C(i = \frac{T}{\Delta t}, j) = (S(i = \frac{T}{\Delta t}, j) - K)_+ \qquad [III.25]$$

According to the fundamental theorem of asset pricing:

$$C(t, S_t, K) = \mathbb{E}^{\mathbb{Q}}\left[e^{-r(T-t)}(S_T - K)_+ | \mathscr{F}_t\right] \qquad [III.26]$$

In order to compute the price of the call option, it is then sufficient to proceed in a backward manner, starting from the terminal nodes where the payoff is known, towards the nodes to the left (and in particular towards the initial node). In other words, the tree (discrete time representation) for the call price process is built in a backward manner starting from the terminal nodes where the payoff is known and using the risk neutral branching probabilities. The risk free rate discount factor is applied at each time step Δt. Let us denote C(i,j) the call price computed at node (i,j). From [III.25], we already know the terminal payoffs $C(i = \frac{T}{\Delta t}, j)$.

In practice, if the node (i,j) corresponds to the standard branching (a) of fig. 5, we have

$$C(i,j) = exp(-r\Delta t) * [p_u(i,j)C(i+1,j+1) + p_m(i,j)C(i+1,j) + p_d(i,j)C(i+1,j-1)] \qquad [III.27]$$

Similarly, if the node (i,j) corresponds to the upward branching (b) of fig. 5, we have

$$C(i,j) = exp(-r\Delta t) * [p_u(i,j)C(i+1,j+2) + p_m(i,j)C(i+1,j+1) + p_d(i,j)C(i+1,j)] \qquad [III.28]$$

Finally, if the node (i,j) corresponds to the downward branching (c) of fig. 5, we have

$$C(i,j) = exp(-r\Delta t) * [p_u(i,j)C(i+1,j) + p_m(i,j)C(i+1,j-1) + p_d(i,j)C(i+1,j-2)] \qquad [III.29]$$

In particular, one can retrieve the price $C(0, S_0, K)$ when we reach $C(i = 0, j = 0)$.

3.3.2 Results and convergence

A trinomial tree uses a constant time step Δt. One must now discuss the question of how to elicit an appropriate Δt. In order to do so, a convergence study must be carried out.

Such a convergence study is illustrated in fig. 6. For a particular strike K=90$, we constructed several trees, each one of them having a constant Δt, but for Δt tending towards zero. As $\Delta t \to 0$, the number of nodes in the tree is growing just as the computation time (as well as the memory requirements in the current implementation of the code). The procedure of section 3.3.1 was then applied to any such tree in order to retrieve a numerical approximation of the price $C(0, S_0, K = 90)$ of the European call option on the barrel of oil, at time $t = 0$ (February 04, 2022) and for the parameters of section 3.1. In fig. 6, the analytical price [III.15] for K=90$ (towards which the trinomial price should converge) was also plotted. This analytical price corresponds to the point of fig. 4 associated to K=90$.

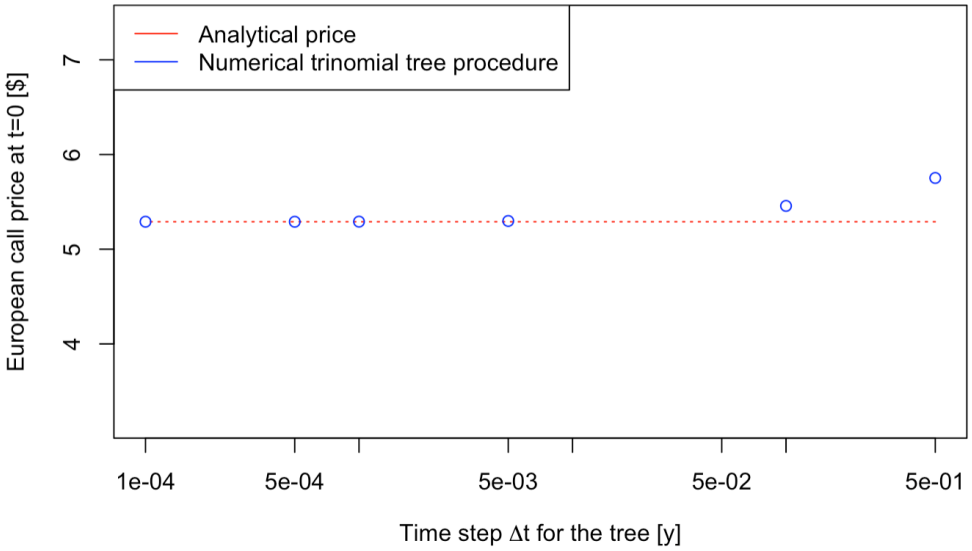

Figure 6: For a strike K=90$ and for the parameters given in section 3.1, numerical trinomial tree price of the European call option on the barrel of oil, at time t=0 (February 04, 2022), as a function of the time step Δt of the tree. The analytical price is also given in dotted lines.

In fig. 6, one can indeed notice that the numerical trinomial price converges towards the analytical price as the time step tends to zero, as it should. This is the expected result since the discrete time approximation provided by the tree converges to the continuous representation for a decreasing time step. Of course, the analytical price is here available, so that the convergence is highlighted more easily. In a situation where an analytical price is not available (or if we do not want to compute the analytical price even if it is available), one could check that the numerical price reaches a stable level for smaller and smaller time steps. Depending on the degree of convergence required, one could then select the appropriate time step: it would be the time step for which no significant improvement is brought (w.r.t. the degree of convergence required) when a smaller Δt is envisioned. In the present case, the price was observed to be converged up to the fourth decimal for $\Delta t = 10^{-4} y$..

Finally, one can plot the converged trinomial prices $C(0, S_0, K)$ for the European call option on the barrel of oil, at time $t = 0$ (February 04, 2022) and for the parameters of section 3.1. This was done in fig. 7, for several strikes. The procedure of section 3.3.1 was applied in all cases with $\Delta t = 10^{-4} y$.. We have just seen that this leads to a reasonable convergence level for K=90$. We assume here that the convergence is equally appropriate for the other strike levels studied. Strictly speaking, the degree of convergence reached could be different for any change in the parameters (including the strike). One would have to properly assess the level of convergence in all those cases with a separate convergence study. Yet, the analytical price [III.15] towards which we should converge was again plotted in fig. 7. The convergence seems again reasonable, providing confidence in our implementation.

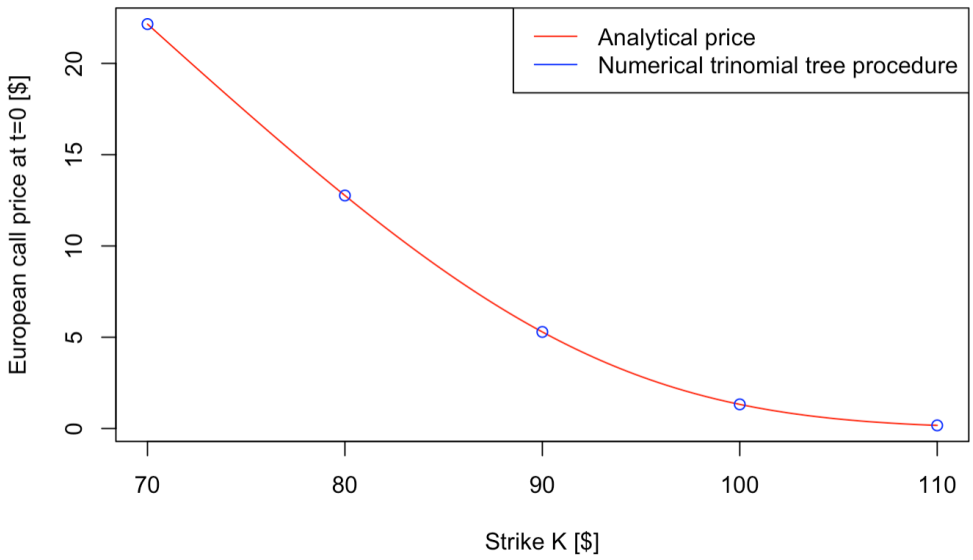

Figure 7: For several strikes K and for the parameters given in section 3.1, numerical trinomial tree prices of the European call option on the barrel of oil, at time t=0 (February 04, 2022), for a time step $\Delta t = 10^{-4}y.$. The analytical price is also given in plain lines.

3.4 Pricing with Monte Carlo simulation and its convergence

3.4.1 Pricing methodology

We will now price numerically the European call option on the mean reverting commodity by implementing a Monte Carlo (MC) simulation. The methodology and notations are quite similar to the ones proposed for question 1 section 2.3. A MC simulation (or MC run) is again defined by a number N of scenarios (or paths), upon which the averaging will be performed, and by a constant time step Δt for the sampling. Within a MC run, N paths are sampled for the underlying barrel of oil by exploiting its risk neutral dynamics [III.1].

Since W_t is a brownian motion under $\mathbb{Q}$ with independent successive increments (normally distributed, with zero mean and variance proportional to time), a discrete time version of the risk neutral dynamics [III.1] for the commodity is given by:

$$\Delta S^{(i)}(j) = \alpha \left(\theta - S^{(i)}(j-1)\right) \Delta t + \sigma.\sqrt{\Delta t}.u^{(i)}(j) \qquad [III.30]$$

$$S^{(i)}(j) = S^{(i)}(j-1) + \Delta S^{(i)}(j) \qquad [III.31]$$

for $j = 1, 2, ..., \frac{T}{\Delta t}$, starting from $S^{(i)}(0) = S_0$ and where $u^{(i)}(j)$ are independent random samples from a $\mathcal{N}(0,1)$. This sampling is performed for each scenario $i = 1, 2, ..., N$. A MC run produces thus N sampled call payoffs $P^{(i)}$ at maturity (for $i = 1, 2, ..., N$) :

$$P^{(i)} = \left(S^{(i)}(j = \frac{T}{\Delta t}) - K\right)_+ \qquad [III.32]$$

This sample distribution approximates the true risk neutral distribution of the call payoff at maturity. As such, in the fundamental theorem of asset pricing, the expectation over $\mathbb{Q}$ can be replaced by a sample average over the N sampled payoffs (discounted at the risk free rate):

$$C(0, S_0, K) = \mathbb{E}^{\mathbb{Q}}\left[e^{-rT}(S_T - K)_+ | \mathscr{F}_0\right] \approx \frac{1}{N}\sum_{i=1}^{N} e^{-rT} P^{(i)} \qquad [III.33]$$

Let us note that the current implementation relies on a finite Δt (cf. [III.30] and [III.31]) and will require a double convergence study (for $\Delta t \to 0$ and for $N \to +\infty$). An alternative would be here to exploit directly [III.10] (giving the risk neutral distribution of S_T at maturity as seen from $0 \leq t \leq T$). For $i = 1, 2, ..., N$, instead of following the underlying over time steps Δt until maturity, one could directly sample the value $S_T^{(i)}$ at maturity, deduce a payoff for the call [III.32] and apply [III.33] for the call pricing. This would accelerate significantly the convergence and would only require a convergence study in the number N of scenarios for the simulation. It would only be possible since an analytical expression such as [III.10] is here available, which is not always the case. Also, in case a barrier condition had been in force (such as in question 1), one would have had anyway to follow the underlying over time with a finite Δt sampling. Our finite Δt implementation appears thus more robust to extra barrier conditions, does not require any analytical expression for the underlying distribution and will enable us to check the analytical formula [III.15], even if the convergence will be delayed.

The sample average [III.33] could be computed by storing all the payoffs $P^{(i)}$ (for $i = 1, 2, ..., N$), by performing the summation and then dividing by N. However, this is not practical numerically for $N \to +\infty$. This would indeed increase the memory requirements and the result of the summation could exceed the internal numerical representation of the computer for N large enough. This is why the average is computed in a more efficient fashion:

$$MC(k+1) = \frac{1}{k+1} \sum_{i=1}^{k+1} e^{-rT} P^{(i)} = \frac{1}{k+1} \left[k . \frac{1}{k} \sum_{i=1}^{k} e^{-rT} P^{(i)} + e^{-rT} P^{(k+1)} \right] = \frac{1}{k+1} \left[k . MC(k) + e^{-rT} P^{(k+1)} \right] [III.34]$$

Only one value must be stored (the MC estimator MC(k) based on the k first paths sampled). MC(k) can be updated progressively as the paths are sampled (for $k = 1, 2, ..., N$). MC(N) is equivalent to [III.33] and MC(k) does not explode in value for large N.

3.4.2 Results and convergence

As mentioned in section 3.4.1, a double convergence study must be carried out (for $\Delta t \to 0$ and for $N \to +\infty$). Strictly speaking, one should perform those two studies simultaneously. In practice, the convergence in N is studied first for a small enough Δt. It allows to find the number N of scenarios that is appropriate considering the precision requirements. Then, the convergence in Δt is studied for a N large enough. It allows to find the time step Δt that is appropriate considering the precision requirements. We will then assume that the N and Δt found in this manner remains adequate (w.r.t. the precision requirements) when they are used concomitantly.

1. Convergence in N (number of scenarios)
Such a convergence study in N is illustrated in fig. 8. It was conducted for a particular strike K=100$, for the European call option on the barrel of oil, at time t = 0 (February 04, 2022) and for the parameters of section 3.1. For a small enough $\Delta t = 0.01$y., several MC runs were performed using various numbers N of scenarios. As N grows, the computation time is increasing. Since the MC simulation exploits stochastic sampling, for a definite N and a given Δt, some dispersion might still occur across different MC runs. This is why for any N studied, ten MC runs were envisioned, to assess the level of convergence. In fig. 8, the analytical price [III.15] for K=100$ (towards which the MC price should converge) was also plotted. This analytical price corresponds to the point of fig. 4 associated to K=100$.

In fig. 8, one can indeed notice that the numerical MC price converges towards the analytical price as N is increasing. The residual dispersion around the analytical price for the ten MC runs using a given N is reduced for a larger N. Yet, the convergence is rather slow. It is well known that the convergence of MC simulation is driven by $1/\sqrt{N}$. As mentioned earlier (cf. section 3.4.1), the convergence could be accelerated with a direct sampling of the value of the barrel at maturity, resorting to formula [III.10]. This is yet not envisioned in the present report, for the reasons mentioned earlier.

Of course, the analytical price is here available, so that the convergence is highlighted more easily. In a situation where an analytical price is not available (or if we do not want to compute the analytical price even if it is available), one could check that the numerical price reaches a stable level and a finer dispersion for larger and larger N. Depending on the degree of convergence required, one could then select the appropriate N. In the present case, for $N = 30,000$ scenarios, the price was observed to be converged only up to the second decimal.

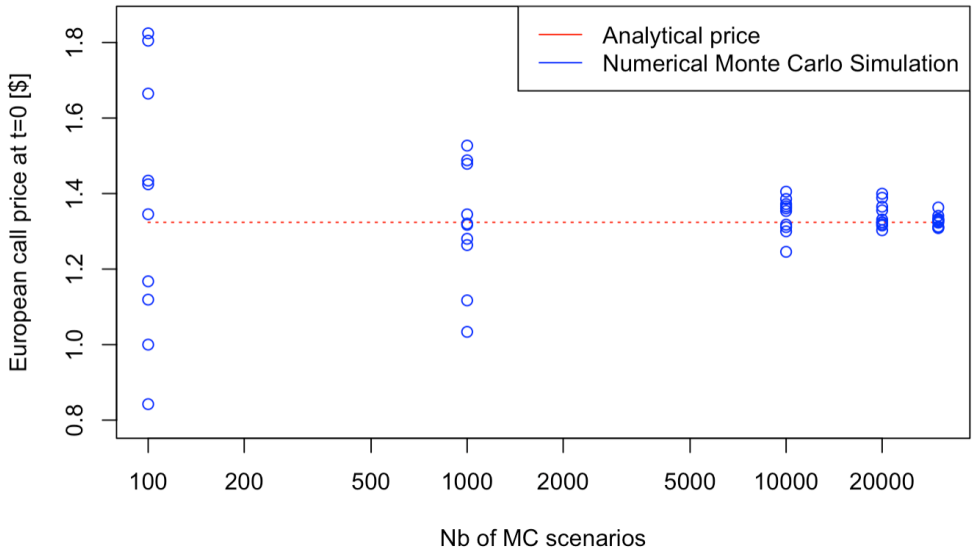

Figure 8: For a strike K=100$ and for the parameters given in section 3.1, numerical MC price of the European call option on the barrel of oil, at time t=0 (February 04, 2022), as a function of the number N of scenarios for the MC simulation. The analytical price is also given in dotted lines.

2. Convergence in Δt (time step)

Such a convergence study in Δt was illustrated in fig. 9. It was conducted for a particular strike K=100$, for the European call option on the barrel of oil, at time t = 0 (February 04, 2022) and for the parameters of section 3.1. For a large enough $N = 10,000$, several MC runs were performed using various time steps Δt. As Δt is reduced, the computation time is increasing. Since the MC simulation exploits stochastic sampling, for a definite N and a given Δt, some dispersion might still occur across different MC runs. This is why for any Δt studied, ten MC runs were envisioned, to assess the level of convergence. In fig. 9, the analytical price [III.15] for K=100$ (towards which the MC price should converge) was also plotted. This analytical price corresponds to the point of fig. 4 associated to K=100$.

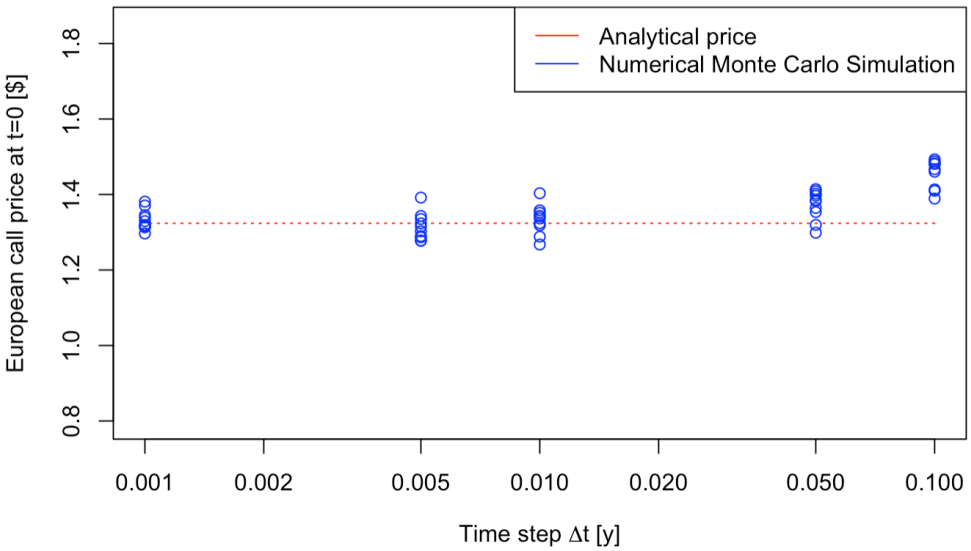

Figure 9: For a strike K=100$ and for the parameters given in section 3.1, numerical MC price of the European call option on the barrel of oil, at time t=0 (February 04, 2022), as a function of the time step Δt for the MC simulation. The analytical price is also given in dotted lines.

The main effect of Δt lies in the mean level around which the ten MC runs are dispersed. In fig. 9, one can indeed notice that the numerical MC price converges towards the analytical price as Δt is reduced, since the mean level of the ten MC runs converges towards the analytical price. This is an expected result since the discrete time approximations [III.30] and [III.31] should converge towards the continuous case for smaller and smaller Δt.

Of course, the analytical price is here available, so that the convergence is highlighted more easily. In a situation where an analytical price is not available (or if we do not want to compute the analytical price even if it is available), one could check that the numerical price reaches a stable level for smaller and smaller Δt. Depending on the degree of convergence required, one could then select the appropriate Δt. In the present case, for $\Delta t = 0.01$y., the price was observed to be converged up to the third decimal.

3. Converged results

Finally, one can plot the converged MC numerical prices $C(0, S_0, K)$ for the European call option on the barrel of oil, at time t = 0 (February 04, 2022) and for the parameters of section 3.1. This was done in fig. 10, for several strikes. In any case, we used $N = 20,000$ scenarios and $\Delta t = 0.01$y.. We have just seen that this leads to a reasonable convergence level for K=100\$. We assume here that the convergence is equally appropriate for the other strike levels studied and when the N and Δt parameters are combined. Strictly speaking, the degree of convergence reached could be different for any change in the parameters (including the strike). One would have to properly assess the level of convergence in all those cases with a separate convergence study. Yet, the analytical price [III.15] towards which we should converge was again plotted in fig. 10. For any strike, ten MC runs were conducted to illustrate the residual stochastic dispersion in the MC estimator. The convergence seems again reasonable, providing confidence in our implementation.

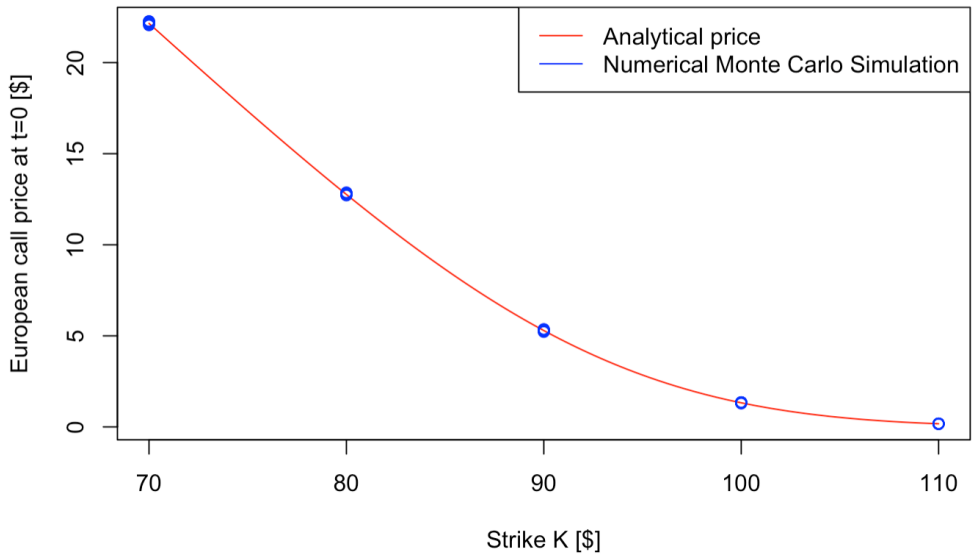

Figure 10: For several strikes K and for the parameters given in section 3.1, numerical MC price of the European call option on the barrel of oil, at time t=0 (February 04, 2022), for $N = 20,000$ scenarios and $\Delta t = 0.01$y.. The analytical price is also given in plain lines.

4. Remark about convergence plots

Providing an analytical price (towards which we should converge) is available, one could use an alternative scale for convergence plots in order to better appreciate the degree of precision reached. It is then common to plot the difference between the numerical and analytical prices, in log scale, as a function of the parameter studied for the convergence. In particular, the log scale gives a better idea of the orders of magnitudes reached for the numerical residuals. Yet, this report only proposes convergence plots under the price scale since the authors estimated they were sufficient to highlight the main effects discussed in the text.

A Appendix: comparison of pricing methodologies

In this report, we studied three different pricing methodologies: the analytical procedure, the numerical trinomial tree as well as the Monte Carlo (MC) numerical simulation. As a conclusion, we will now review some advantages and disadvantages of those pricing techniques.

The analytical formula, when possible, delivers a closed expression for derivatives' prices. Such an approach was permitted considering the model of question 2. Yet, an analytical expression is not always available. If possible, it can be useful to calibrate the model. For instance, an implicit volatility for the assets can be deduced from the analytical price formula and from market prices of the derivatives. However, when the market is dry (such as in question 1), this idea of implicit volatility calibration from market prices is not really helpful given that the derivative is rarely traded. This is why we could only resort to historical volatilities in question 1.
To ensure no mistake was made during the analytical derivation, it might be interesting to apply other pricing methodologies. For instance, in question 2, the trinomial tree and MC numerical prices were observed to converge towards the analytical price. It provided confidence in our multiple implementations.

However, the convergence of numerical techniques can be rather slow, with a quite significant computational burden and memory requirements. This was especially true for the MC simulation in question 1. In that case, the two risk factors (two brownian samplings), the large time horizon (maturity T=2 years) and the necessity to follow the assets over time (to account for the knock-out condition) delayed significantly the convergence. The knock-out condition also enforced us to envision a finite Δt implementation and a double convergence study (on the number N of scenarios and on the time step Δt).
The convergence of the MC simulation in question 2 was also rather slow. In that case, the absence of barrier condition and the analytical distribution [III.10] for the underlying at maturity could accelerate significantly the convergence. Instead of sampling a discrete time path for the underlying, one could have directly sampled the value of the underlying at maturity from [III.10]. A single convergence study (on the number N of scenarios) would then be possible. However, such an idea is not helpful if no analytical distribution is available for the underlying or if a barrier condition is introduced.
In any case, the convergence of a MC simulation is known to be of order $1/\sqrt{N}$ where N is the number of MC scenarios. There exists a wide literature about variance reduction techniques, importance sampling and other MC acceleration procedures but this goes well beyond the scope of this introductory work.

The convergence of the trinomial tree procedure in question 2 was much faster. This is essentially because this numerical technique does not resort the stochastic sampling. A trinomial tree is in particular well adapted to introduce mean reversion effects.

Finally, numerical procedures offer an advantage of simplicity and robustness w.r.t. the not always possible analytical pricing. In a situation where an analytical price is not available (or if we do not want to compute the analytical price even if it is available), one could check when the numerical price reaches a stable level. One could then deduce the appropriate values for the parameters N and/or Δt considering the convergence requirements.

B Appendix: From real measure to risk neutral measure for the model of question 1

Under the real measure $\mathbb{P}$, the model of question 1 is given by:

$$\begin{pmatrix} \frac{dS_t^1}{S_t^1} \\ \frac{dS_t^2}{S_t^2} \end{pmatrix} = \begin{pmatrix} \mu_1 \\ \mu_2 \end{pmatrix} dt + \begin{pmatrix} \sigma_{11} & \sigma_{12} \\ \sigma_{21} & \sigma_{22} \end{pmatrix} \begin{pmatrix} dW_t^1 \\ dW_t^2 \end{pmatrix} = \bar{\mu} dt + \Sigma \begin{pmatrix} dW_t^1 \\ dW_t^2 \end{pmatrix} \qquad dB_t = rB_t dt \qquad [B.1]$$

where $\bar{\mu}$ and Σ are constant real matrices and where W_t^1 and W_t^2 are independent brownian motions under $\mathbb{P}$.

The Radon-Nikodym derivative is given by:

$$\left. \frac{d\mathbb{Q}}{d\mathbb{P}} \right|_t = exp\left[\frac{-1}{2}(\theta_1^2 + \theta_2^2)t - \theta_1 W_t^1 - \theta_2 W_t^2 \right] \qquad [B.2]$$

We have:

$$dW_t^{1\mathbb{Q}} = dW_t^1 + \theta_1 dt \qquad dW_t^{2\mathbb{Q}} = dW_t^2 + \theta_2 dt \qquad [B.3]$$

where $W_t^{1\mathbb{Q}}$ and $W_t^{2\mathbb{Q}}$ are independent brownian motions under $\mathbb{Q}$.

As such, under $\mathbb{Q}$, we have:

$$\begin{pmatrix} \frac{dS_t^1}{S_t^1} \\ \frac{dS_t^2}{S_t^2} \end{pmatrix} = \begin{pmatrix} \mu_1 \\ \mu_2 \end{pmatrix} dt + \begin{pmatrix} \sigma_{11} & \sigma_{12} \\ \sigma_{21} & \sigma_{22} \end{pmatrix} \begin{pmatrix} dW_t^{1\mathbb{Q}} - \theta_1 dt \\ dW_t^{2\mathbb{Q}} - \theta_2 dt \end{pmatrix} = \begin{pmatrix} \mu_1 - \sigma_{11}\theta_1 - \sigma_{12}\theta_2 \\ \mu_2 - \sigma_{21}\theta_1 - \sigma_{22}\theta_2 \end{pmatrix} dt + \begin{pmatrix} \sigma_{11} & \sigma_{12} \\ \sigma_{21} & \sigma_{22} \end{pmatrix} \begin{pmatrix} dW_t^{1\mathbb{Q}} \\ dW_t^{2\mathbb{Q}} \end{pmatrix} [B.4]$$

We conclude that the risk premiums θ_1 and θ_2 must satisfy the following relations:

$$r = \mu_1 - \sigma_{11}\theta_1 - \sigma_{12}\theta_2 \qquad r = \mu_2 - \sigma_{21}\theta_1 - \sigma_{22}\theta_2 \qquad [B.5]$$

or under the matrix formalism

$$\begin{pmatrix} r \\ r \end{pmatrix} = \bar{\mu} - \Sigma \begin{pmatrix} \theta_1 \\ \theta_2 \end{pmatrix} \qquad [B.6]$$

It implies that the risk premiums can indeed be taken as real constants

$$\begin{pmatrix} \theta_1 \\ \theta_2 \end{pmatrix} = \Sigma^{-1} \left[\bar{\mu} - \begin{pmatrix} r \\ r \end{pmatrix} \right] \qquad [B.7]$$

Under the risk neutral measure $\mathbb{Q}$, the dynamics of the stocks becomes thus:

$$\begin{pmatrix} \frac{dS_t^1}{S_t^1} \\ \frac{dS_t^2}{S_t^2} \end{pmatrix} = \begin{pmatrix} r \\ r \end{pmatrix} dt + \begin{pmatrix} \sigma_{11} & \sigma_{12} \\ \sigma_{21} & \sigma_{22} \end{pmatrix} \begin{pmatrix} dW_t^{1\mathbb{Q}} \\ dW_t^{2\mathbb{Q}} \end{pmatrix} \qquad dB_t = rB_t dt \qquad [B.8]$$